JOURNAL OF COMPUTATIONAL PHYSICS 91, 55–70 (1990)

Open Boundary Conditions for External Flow Problems

LARS FERM

Department of Scientific Computing, University of Uppsala, Sturegatan 4B 2tr, S-752 23 Uppsala, Sweden

Received December 6, 1988; revised June 27, 1989

The steady Euler equations are considered. Very accurate open boundary conditions are derived for the external problem when the outer boundary is an ellipse. These conditions have the same algebraic form as the corresponding conditions when the boundary is a straight line across an infinitely long channel. A new implementation is introduced for the external problem. At every time step a matrix is applied on a vector containing values from every grid point at the boundary. The computational work for these calculations is kept low by introducing a special set of fewer boundary condition points. Experiments demonstrate the accuracy of the boundary procedure. © 1990 Academic Press, Inc.

1. INTRODUCTION

Artificial boundaries are often introduced when partial differential equations are to be solved numerically over unbounded regions. It is natural that no data are available at such a boundary, but data are needed to make the problem well posed. A simple procedure is to use such a large computational region that the free stream values can be used as good approximations to the solution at the boundary. If the computational region is not that large, more accurate boundary conditions must be used. Engquist and Majda [2, 3] derive a hierarchy of boundary conditions for the time-dependent problem. The principle is that the out-going waves should pass the boundary without leaving reflections back into the computational domain. The first approximation of the hierarchy is to set the in-going characteristic variables to the free stream values. That procedure has often been used for steady-state calculations, but again the computational region must be so large that these characteristic variables approximately take the free stream values at the boundary. Bayliss and Turkel [1] also derive boundary conditions by approximating the out-going waves. Gustafsson [7] generalizes the conditions by Engquist and Majda taking into account waves from the outside. His conditions are intended for the time-dependent problem.

In this paper we derive conditions for the steady Euler equations when the outer boundary is an ellipse. The great advantage of the boundary conditions presented here is the accuracy, which makes it possible to use a relatively small computational

0021-9991/90 $3.00

region. The problem considered here is to find the steady-state solution that matches the free stream data. Thus the converged solution should be independent of the initial one which we otherwise do not know how to choose.

Only the steady-state equations will be considered when the boundary conditions are constructed here. The only approximation introduced is the freezing of the coefficient matrices of the differential equations. The fundamental solution of the constant coefficient problem obtained is constructed, and the form of this solution leads to the boundary conditions. Since the boundary conditions are satisfied exactly by the fundamental solution, they will be called the fundamental boundary conditions. The method has already been developed for flow in a channel and when the flow is periodic in one of the cartesian coordinates [4, 5]. It is based on an idea given by Gustafsson and Kreiss [8]. Fix and Marin [6] propose a similar technique for the Helmholz equations. Hagstrom and Keller [9] discuss this type of boundary conditions from a general point of view. The boundary conditions are derived in Section 2. They are expressed as relations between the Fourier coefficients of the solution, but in the external case no Fourier transformations are carried out explicitly in a practical calculation. The implementation of the boundary conditions is described in Section 3. The accuracy of the boundary conditions is demonstrated by numerical experiments presented in Section 4. The program used for the computations in the interior has been developed at the FFA, Stockholm, Sweden, by A. W. Rizzi and L. E. Eriksson. Some conclusions are given in Section 5.

2. Construction of the Boundary Conditions

Consider the flow around an object like an airfoil, and introduce an ellipse as an artificial boundary around it. We assume that there are no discontinuities of the flow in the area outside the boundary. The construction of the boundary conditions depends only on the properties of the solution outside the ellipse. Thus discontinuities are allowed in the interior of the computational domain. The steady Euler equations are

$$Aw_x + Bw_y = 0, \tag{1}$$

where

$$w = \begin{pmatrix} \rho \\ u \\ v \\ p \end{pmatrix},$$

$$A = \begin{pmatrix} u & \rho & 0 & 0 \\ 0 & u & 0 & 1/\rho \\ 0 & 0 & u & 0 \\ 0 & c^2\rho & 0 & u \end{pmatrix}, \qquad B = \begin{pmatrix} v & 0 & \rho & 0 \\ 0 & v & 0 & 0 \\ 0 & 0 & v & 1/\rho \\ 0 & 0 & c^2\rho & v \end{pmatrix}.$$

To construct the boundary conditions we introduce the constant free stream values denoted by $\bar{\rho}, \bar{u}, \bar{v}, \bar{p}, \ldots$ into the coefficient matrices of the differential equations. By choosing a coordinate system with the x-axis parallel to the free stream direction, we get the condition

$$\bar{v} = 0.$$

Thus the rank of the frozen matrix B is two, and hence the derivatives with respect to y can be eliminated from two equations. We get

$$\frac{\partial}{\partial x}\begin{pmatrix} p + \bar{\rho}\bar{u}u \\ p - \bar{c}^2\rho \end{pmatrix} = 0. \tag{2}$$

These equations lead to the local boundary conditions

$$\begin{aligned} p + \bar{\rho}\bar{u}u &= \bar{p} + \bar{\rho}\bar{u}^2 \\ p - \bar{c}^2\rho &= \bar{p} - \bar{c}^2\bar{\rho}. \end{aligned} \tag{3}$$

The frozen differential equations also lead to the system

$$\frac{\partial}{\partial x_1}\begin{pmatrix} v \\ \eta p \end{pmatrix} + \begin{pmatrix} 0 & 1 \\ -1 & 0 \end{pmatrix}\frac{\partial}{\partial y}\begin{pmatrix} v \\ \eta p \end{pmatrix} = 0, \tag{4}$$

where

$$\begin{aligned} \eta &= \sqrt{\bar{c}^2 - \bar{u}^2}/\bar{c}\bar{\rho}\bar{u}, \\ x_1 &= x/\eta\bar{\rho}\bar{u}. \end{aligned} \tag{5}$$

These are the Cauchy–Riemann equations for the analytic function

$$f(z) = \eta p + iv, \tag{6}$$

where

$$z = x_1 + iy.$$

Since the limit at infinity exists, the analytic function can be expanded in the power series

$$f(z) = \sum_{\omega=0}^{\infty} a_\omega z^{-\omega},$$

or equivalently,

$$f = \sum_{\omega=0}^{\infty} \frac{1}{r^\omega}\left[b_\omega \cos \omega\phi + c_\omega \sin \omega\phi\right] + i \sum_{\omega=0}^{\infty} \frac{1}{r^\omega}\left[c_\omega \cos \omega\phi - b_\omega \sin \omega\phi\right], \tag{7}$$

where

$$z = re^{i\phi},$$
$$a_\omega = b_\omega + ic_\omega.$$

On the other hand, we introduce the Fourier expansions of p and v,

$$w = \begin{pmatrix} p \\ v \end{pmatrix} = \sum_{\omega=-\infty}^{\infty} \hat{w}_\omega(r)\, T_\omega(\phi), \tag{8}$$

where

$$T_\omega(\phi) = \begin{cases} \cos \omega\phi & \text{for} \quad \omega \geqslant 0, \\ \sin \omega\phi & \text{for} \quad \omega < 0, \end{cases}$$

into definition (6) of the analytic function $f(z)$. Identfying the terms obtained to those of expansion (7), we get for $\omega \neq 0$

$$\begin{aligned} \eta\hat{p}_\omega(r) + \hat{v}_{-\omega}(r) &= 0, \\ \eta\hat{p}_{-\omega}(r) - \hat{v}_\omega(r) &= 0. \end{aligned} \tag{9}$$

The terms for $\omega = 0$ in expansion (7) are independent of r. Thus we obtain the conditions

$$\begin{aligned} \hat{p}_0(r) &= \lim_{\xi \to \infty} \hat{p}_0(\xi) = \bar{p}, \\ \hat{v}_0(r) &= \lim_{\xi \to \infty} \hat{v}_0(\xi) = \bar{v} = 0. \end{aligned} \tag{10}$$

Conditions (9) and (10) are valid on circles enclosing the computational domain. They are thus valid as boundary conditions in the special case when the boundary in the z-plane is a circle. Furthermore, they are also valid as boundary conditions if the exterior region in the z-plane can be mapped analytically onto the region outside a circle. This follows since we only used the analyticity of the function $f(z)$.

Assume that the boundary in the original (x, y)-plane is a circle. The rescaling (5) of the x-axis leads to an ellipse in the z-plane of the form

$$\begin{pmatrix} x_1 \\ y \end{pmatrix} = D \begin{pmatrix} \cos\phi \\ \sin\phi \end{pmatrix}, \tag{11}$$

where

$$D = \operatorname{diag}(d_i), \qquad d_i > 0.$$

By introducing the unit circle

$$w = e^{i\phi}$$

into the equation

$$z = \frac{d_1 + d_2}{2} w + \frac{d_1 - d_2}{2} \frac{1}{w}, \tag{12}$$

we obtain the ellipse (11) in the z-plane. Equation (12) can be regarded as quadratic for w, and the two roots satisfy the condition

$$|w_1 w_2| = \left| \frac{d_1 - d_2}{d_1 + d_2} \right| < 1.$$

Hence there is only one root outside the unit circle in the w-plane. Thus Eq. (12) defines an analytic mapping of the exterior region in the z-plane onto the region outside the unit circle in the w-plane. Hence boundary conditions (9) and (10) are valid for the Fourier coefficients with respect to ϕ.

For some problems one might prefer a general ellipse as the artificial boundary in the original (x, y)-plane

$$\begin{pmatrix} x \\ y \end{pmatrix} = RD \begin{pmatrix} \cos\theta \\ \sin\theta \end{pmatrix}, \tag{13}$$

where the matrix D is diagonal as in (11), and R is a rotational matrix needed when the free stream direction is not parallel to one of the axes of the ellipse. The boundary in the z-plane is also an ellipse, and a corresponding representation of it is introduced:

$$\begin{pmatrix} x_1 \\ y \end{pmatrix} = R_1 D_1 \begin{pmatrix} \cos\phi \\ \sin\phi \end{pmatrix}. \tag{14}$$

A rotation of the z-plane gives the ellipse the form (11), and, as above, it is transformed to the unit circle with the parameter ϕ as the angular coordinate. A relation between the parameters θ and ϕ is obtained from Eqs. (5), (13), (14):

$$\begin{pmatrix} \cos\theta \\ \sin\theta \end{pmatrix} = M \begin{pmatrix} \cos\phi \\ \sin\phi \end{pmatrix}. \tag{15}$$

Being constant, the matrix M must have the form

$$M = \begin{pmatrix} \cos\psi & \sin\psi \\ \pm\sin\psi & \mp\cos\psi \end{pmatrix},$$

where ψ is a constant angle. Thus Eq. (15) leads to the condition

$$\phi = \begin{matrix} + \\ (-) \end{matrix} (\theta - \psi).$$

The minus sign is omitted since θ and ϕ are assumed to run in the same direction around the boundary. Thus a rotation of the w-plane gives the boundary the form

$$w_1 = e^{i\theta}.$$

Since only analytic mappings are involved, the boundary conditions are valid for the Fourier coefficients with respect to θ. Hence the different mappings used in the derivation of the boundary conditions can be disregarded in practise. Only representation (13) of the original ellipse is needed. It can be pointed out that the technique used in this section is applicable for the channel problems studied in [4, 5]. The unbounded regions are semi-infinite strips, and thus exponential functions can be used as the required analytic mappings.

In the computations presented in Section 4 we will only treat flow with constant stagnation enthalpy h_0, so that for a perfect gas the Bernoulli equation

$$p = \frac{\gamma - 1}{2\gamma} \rho(2h_0 - u^2 - v^2),$$

replaces the last one of the four Eqs. (1). Thus we can eliminate the derivatives of the pressure from the remaining three equations using the chain rule. By linearizing the thus reduced system we obtain the systems (2) and (4) with p replaced by $\bar{c}^2\rho$, where $\bar{c}^2 = \gamma\bar{p}/\bar{\rho}$. The second Eq. (2) is omitted. Thus the second condition (3) will not be tested experimentally here, but it was used in [4] for flow in a channel with solid walls.

3. Implementation of the Boundary Conditions

Conditions (3), (9), and (10) form a complete set of boundary conditions for the differential equations, but extra numerical conditions are needed for the discretized problem. The numerical conditions considered here are extrapolations from the interior of the out-going characteristic variables of the time-dependent problem. These characteristic variables correspond to the linearized one-dimensional problem in the direction perpendicular to the boundary. Other linear boundary conditions can be treated similarly.

At an outflow point there are three out-going characteristic variables. At an inflow point there is only one, but we add the two local conditions (3). Thus there are three local conditions at every boundary point. The discrete boundary values are denoted by ρ_j, u_j, v_j, and p_j, $j = 1, ..., N$, where N is the number of boundary

points. We eliminate u_j and ρ_j from these three conditions, and get a local condition for p_j and v_j only,

$$a_j p_j + b_j v_j = h_j, \qquad j = 1, 2, ..., N. \tag{16}$$

For flow in a channel with solid walls it is natural to use a straight line across the channel as an artificial boundary. Thus the boundary is perpendicular to the free stream direction. It turns out that the characteristic variables take such a form that the coefficients a_j are zero at the outflow boundary, and the coefficients b_j are zero at the inflow boundary. Hence one of the variables p_j and v_j can be determined using local conditions only. By Fourier transforming this variable along the boundary, the global conditions can be applied explicitly. The obtained values are transformed back to the physical space.

The boundary conditions are also applicable when the problem is periodic in one of the cartesian coordinates, and the boundary is a straight line in the periodic direction. We cannot assume that the free stream direction is perpendicular to this boundary, and hence usually not calculate p_j or v_j using the local conditions only. However, by linearizing around the same state at all points when defining the characteristic variables, the coefficients a_j and b_j become independent of j. Thus the Fourier coefficients of p or v can be determined from those of h, and hence the procedure becomes similar to that of the channel problem.

If the boundary is an ellipse, the characteristic variables are different linear combinations of the physical ones at different points at the boundary. Thus a new technique is needed.

We let the vectors $\mathbf{p}_1$ and $\mathbf{v}_1$ contain the values of p and v at those points where $|a_j| \leqslant |b_j|$. The remaining values are stored in vectors $\mathbf{p}_2$ and $\mathbf{v}_2$. Thus we may assume that the local conditions (16) have the form

$$\begin{pmatrix} \mathbf{v}_1 \\ \mathbf{p}_2 \end{pmatrix} = G \begin{pmatrix} \mathbf{p}_1 \\ \mathbf{v}_2 \end{pmatrix} + \mathbf{h}, \tag{17}$$

where G is a diagonal matrix and the vector $\mathbf{h}$ contains the values h_j determined locally. We write the global conditions (9) and (10) as

$$B_1 \hat{\mathbf{p}} + B_2 \hat{\mathbf{v}} = \mathbf{q}_0,$$

where B_1 and B_2 are $N \times N$-matrices, and the vectors $\hat{\mathbf{p}}$ and $\hat{\mathbf{v}}$ contain the Fourier coefficients of the finite expansions corresponding to (8). The vector $\mathbf{q}_0$ contains only zeros but for the element $\bar{p}$ from condition (10). The corresponding conditions for the physical variables are

$$B_1 F \begin{pmatrix} \mathbf{p}_1 \\ \mathbf{p}_2 \end{pmatrix} + B_2 F \begin{pmatrix} \mathbf{v}_1 \\ \mathbf{v}_2 \end{pmatrix} = \mathbf{q}_0, \tag{18}$$

where F is the Fourier matrix relating the physical and Fourier spaces. These conditions can also be written as

$$B_3 \begin{pmatrix} \mathbf{p}_1 \\ \mathbf{v}_2 \end{pmatrix} + B_4 \begin{pmatrix} \mathbf{v}_1 \\ \mathbf{p}_2 \end{pmatrix} = \mathbf{q}_0. \tag{19}$$

Introducing the local conditions (17), we get

$$\begin{pmatrix} \mathbf{p}_1 \\ \mathbf{v}_2 \end{pmatrix} = C\mathbf{h} + \mathbf{q}, \tag{20}$$

where

$$C = -B_5^{-1} B_4$$
$$\mathbf{q} = B_5^{-1} \mathbf{q}_0$$
$$B_5 = B_3 + B_4 G.$$

Condition (20) is applied at every time step when the local values $\mathbf{h}$ have been calculated. The remaining variables are then determined using the local conditions.

Calculation of the matrix C involves matrix operations which are too large to be carried out every time step. The matrix is determined by the matrices in condition (19), and by the coefficients a_j and b_j of the local conditions (16). The former are independent of time but the latter are changed when the flow switches between an inflow and an outflow state. Hence the local conditions must be modified at those critical points where that might happen. The outflow and inflow states have one local condition in common, since one of the characteristics always leaves the computational domain. We modify this common condition at the critical points by setting the coefficient for u_j to zero in the definition of the extrapolated variable. The coefficient for ρ_j is zero from the beginning. Thus the common condition takes the form (16), and hence the coefficients a_j and b_j are independent of the other two local conditions. Those points where the angle between the velocity vector and the tangent of the boundary is small, are treated as critical points. If the flow during the computation switches between inflow and outflow at a non-critical point, the matrix C must be regenerated. That problem did not appear in the experiments presented below. When the flow is close to the steady state, the limit angle for classing a point as critical can be reduced. In the experiments the limit angle was set proportional to the residual, and the number of critical points was reduced once or twice during the computation. Finally, no points were treated as critical.

The matrix F in condition (18) is the usual Fourier matrix if the boundary points are uniformly spaced with respect to the angular coordinate describing the boundary. If the boundary points are not uniformly spaced, we can still easily express the physical variables in terms of the Fourier coefficients. Thus the matrix F can be calculated using a matrix inversion. However, when this technique was tested in practise, the resulting boundary conditions did not work at all. Thus

another method is needed. A simple procedure that works well is to use two sets of boundary points, one containing the boundary points of the interior grid and one containing uniformly spaced points for the boundary conditions. Local polynomial interpolations transfer the solution back and forth between the two point sets. Values at four gridpoints are used for these interpolations in most of the experiments presented in the next section. A great advantage of this method is that the number of boundary condition points can be chosen independently of the grid in the interior. Thus the order of the matrix C can be reduced by using fewer boundary condition points.

We summarize the boundary procedure.

Choose a set of uniformly spaced boundary points. They can be chosen independently of the grid in the interior. Construct the matrix C and the vector $\mathbf{q}$ in condition (20) as described above. The calculations every time step are

1. Extrapolate the solution from the interior to the boundary.
2. Interpolate the solution locally to the uniformly spaced boundary condition points.
3. Use the interpolated values to calculate the vector $\mathbf{h}$ in condition (17), and apply the matrix C. One value, p_j or v_j, is thus obtained at every boundary point.
4. Calculate the remaining values at these points using the local conditions.
5. Interpolate the solution back to the original boundary points.
6. Calculate the final boundary values using the step 1-values for the outgoing characteristic variables, and the step 5-values for the in-going ones.

It has turned out that the last step improves the convergence rate slightly. The implementation described above is applicable for the reduced problem mentioned at the end of the preceding section if p is replaced by ρ. We eliminate u_j from two local conditions at every boundary point to get one condition for ρ_j and v_j only.

4. Numerical Experiments

The only approximation introduced when the boundary conditions are constructed is the freezing of the coefficient matrices of the differential equations. The experiments presented in this section demonstrate the accuracy of the procedure for the true non-linear problem.

The boundary conditions are introduced into a program developed at the FFA, Stockholm, Sweden by A. W. Rizzi. The program is built up by a time-dependent finite-volume method with a multi-stage explicit scheme in time [10]. The meshes are generated by L. E. Eriksson's (FFA) transfinite interpolation program. As mentioned above the pressure is eliminated from the system assuming constant stagnation enthalpy.

As a test problem we consider the flow around a NACA0012 airfoil at a 1° angle

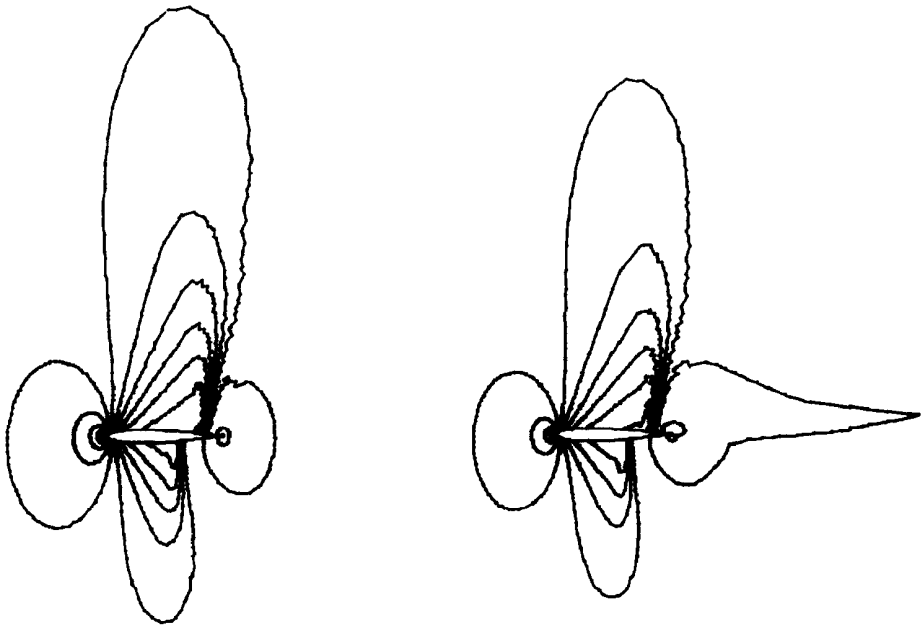

FIG. 1. Level curves of the solution of the test problem: The pressure to the left and the Mach number to the right.

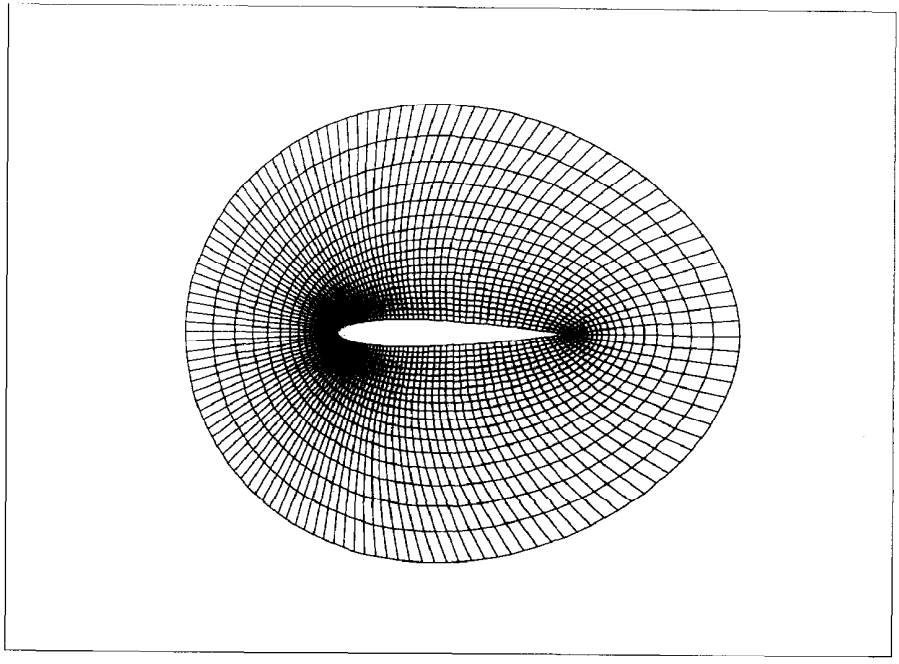

FIG. 2. The type of mesh used in the experiments.

of attack. The free stream Mach number is 0.85. The Mach number and the pressure of the solution are plotted in Fig. 1. The flow is supersonic in an area reaching about 1.8 cord lengths from the airfoil. We expect that the true non-linear equations are needed in that area. A 129×27 grid is generated over a region with radius 2.3 cord lengths with the boundary points given by the intersection between the boundary and the grid lines of a mesh over a larger region. The boundary points are thus not uniformly spaced with respect to the angular coordinate. The region is enlarged by adding new circular grid rings around it. The innermost part of the grid is shown in Fig. 2. New grids are generated over smaller regions with radii 1.5 and 1.9. If the region is decreased further, an ellipse would be advantageous as the outer boundary. The solution of the incompressible equations is smoother, and high accuracy of the boundary conditions can be expected very close to the airfoil. Experiments confirming that have been carried out using an ellipse with eccentricity $\frac{1}{3}$ and the major axis 1.2 ($=2 \times 0.6$) cord lengths. Since the incompressible equations can be solved efficiently by other methods, they will not be considered here.

Three different boundary procedures will be compared

C—The free stream values are used for the characteristic variables corresponding to the in-going characteristics. The differential equations are frozen at the free stream values when the characteristic variables are defined. Values from the interior are used for the out-going characteristic variables.

R—The boundary conditions used by Rizzi in the original program. They are similar to the C-conditions, but the Riemann-invariants of the non-linear equations are used. The accuracy is improved by adding a vortex correction term to the free stream values in the boundary conditions.

F—The fundamental boundary conditions studied here.

Results obtained with these boundary conditions for different sizes of the domain are shown in Fig. 3. The pitch moment, lift, and drag are plotted as functions of the radius. Horizontal lines are drawn through the values obtained using the largest region with $r = 13$. Since the F-results for $r = 4.1$ and $r = 13$ are almost identical, we conclude that the linearized equations approximate the solution well in the region $4.1 < r < 13$. The solution should be smoother outside this region than in the interior. Thus the linearized system should approximate the solution even better for $r > 13$, and hence the F-values at $r = 13$ should be close to the true ones. The vortex correction term of the R-conditions is based on the lift at the surface of the airfoil. A comparision between the C- and R-results indicates that this term improves the lift value considerably. Yet the r-dependency of the lift is about three times less with the F-conditions. Actually the R-lift at $r = 13$ is close to the F-lift at $r = 2$, interpolated from the results for $r = 1.9$ and $r = 2.3$. The errors increase rapidly for all boundary conditions in the supersonic area. Apart from the vortex correction term of the R-conditions, the R-, C-, and F-conditions are equivalent for a constant

solution. The vortex correction term is of the order $1/r$. Thus the three boundary conditions should be equivalent in the limit when the region increases.

As described in the preceding section the order of the matrix C in condition (20) can be reduced by using fewer boundary condition points. Denote the number of those points by N. The effect of reducing N is studied by solving the problem with $N=8$, 16, 32, 64, and 128. We use the grid with radius 2.3 for these calculations. The circulation, pitch moment, drag, and lift are calculated. The results are normalized making the value for $N=128$ equal to 100. They are plotted in Fig. 4. A smoothing operator is introduced at the interpolation between the two point sets for $N=8$, otherwise the solution does not converge. This is the source of most of the large errors shown in the figure for $N=8$. The smoothing operator is not needed for larger values of N, but the number of steps is slightly increased for $N=16$. The experiments indicate that N can be reduced to 32, i.e., by a factor 4 with very little loss of accuracy and convergence rate. Thus the computational work at the boundary is reduced to less than that over one grid ring in the interior.

The experiments presented above show that the F-conditions make it possible to reduce the computational region considerably, and that the computational work at the boundary can be kept low every time step. The total amount of work depends

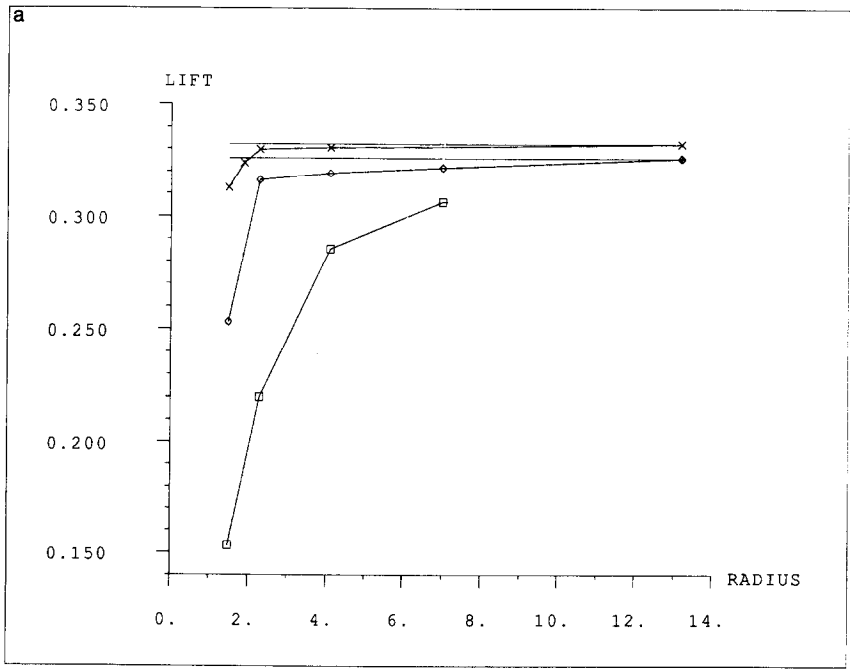

FIG. 3. Results as functions of the radius of the domain for different boundary conditions: □ C-conditions; ◇ R-conditions; × F-conditions. (a) Lift; (b) Drag; (c) Pitch moment.

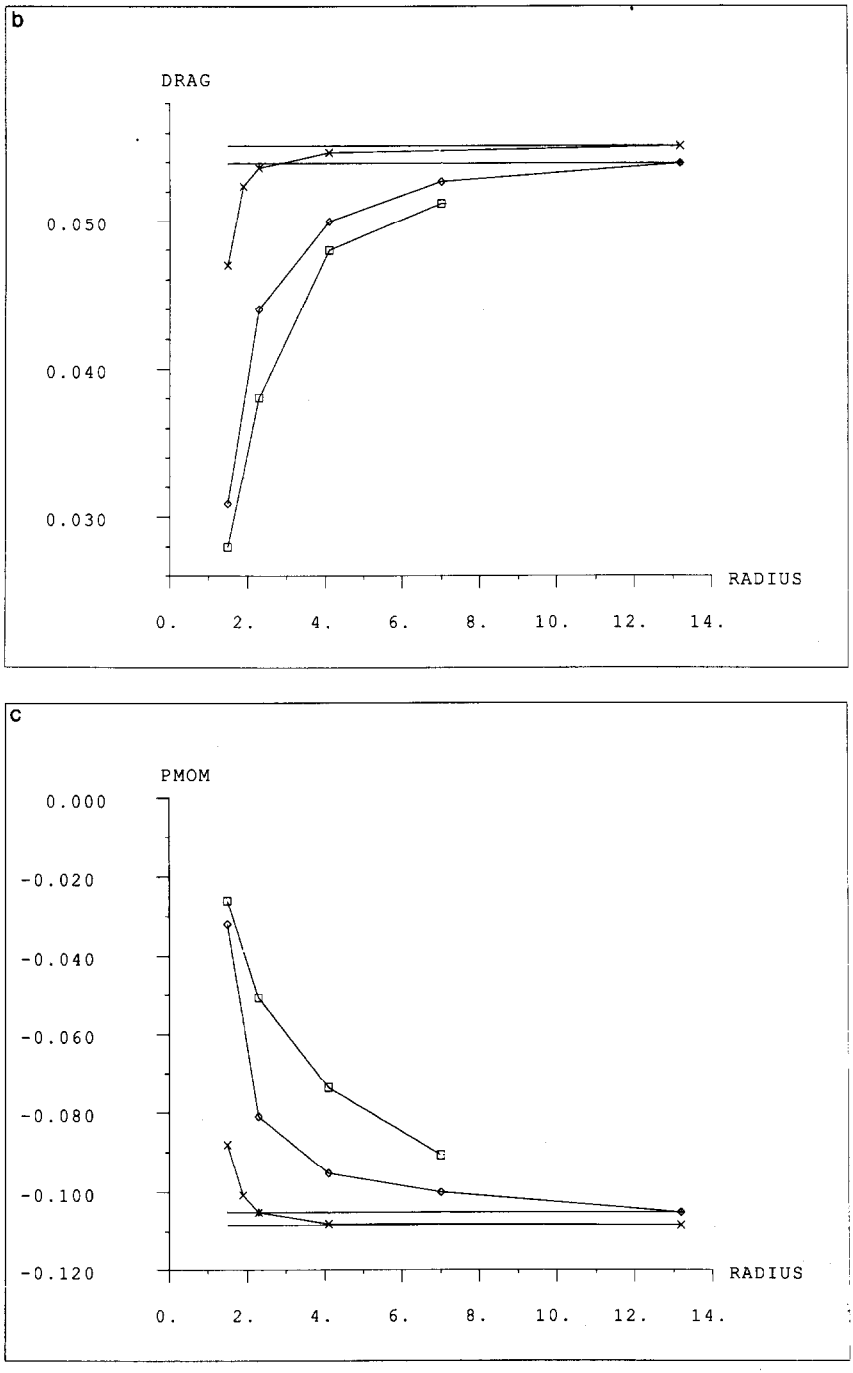

FIG. 3—*Continued*

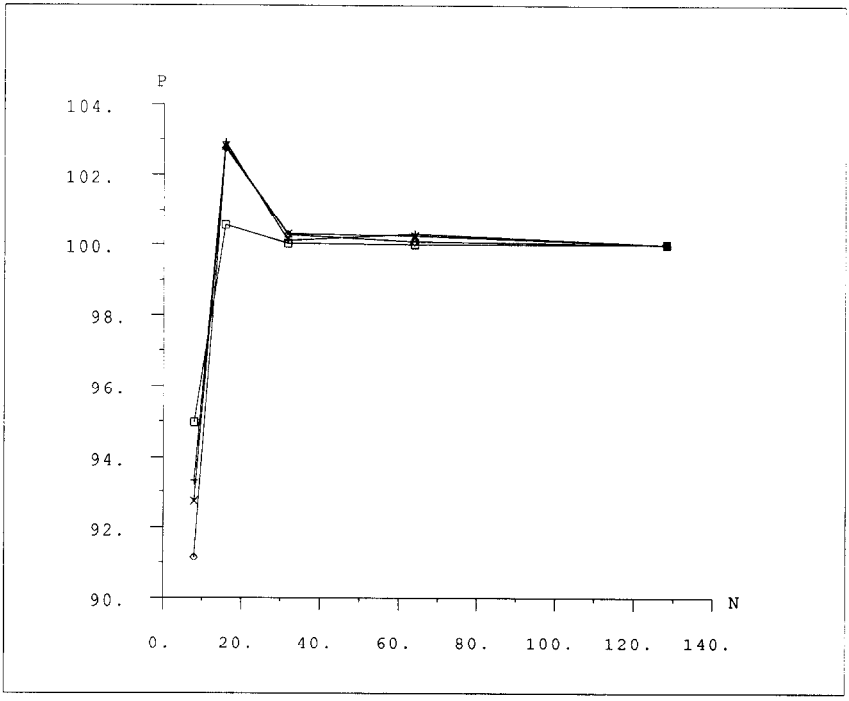

FIG 4. Normalized results for different numbers of boundary condition points: □ Drag × Circulation + Lift; ◇ Pitch moment.

also on the number of grid points needed in the different regions and the number of time steps needed to reach the steady state. We will not optimize the grids here, but it could be interesting to look at the convergence rates with the particular grids used in the calculations presented above. It turns out that the F-conditions delay the convergence to the steady state on a fixed grid. The C-conditions lead to the most rapid convergence. However, when the computational region is decreased, the convergence rate increases again. The F-values at $r = 2.3$ are close to the R-values at $r = 13$ in Fig. 3. Thus it is interesting to compare the number of time steps needed to obtain these results. The grids coincide in the small region. The distance between the grid rings is increased by factor 1.2 for every new ring outside the smaller region. The number of grid rings in the two regions are 27 and 41. The logarithm of the residual is plotted in Fig. 5. The decay rates are obviously very similar. It should be pointed out that these results could be different if the grids were strictly optimized. Thus the amount of saved computational work may not be as large as 30% with such grids. The efficiency of the boundary conditions may also depend on the required accuracy. They seem to be most interesting when high accuracy is important. The efficiency may also be different with another kind of grid, and with

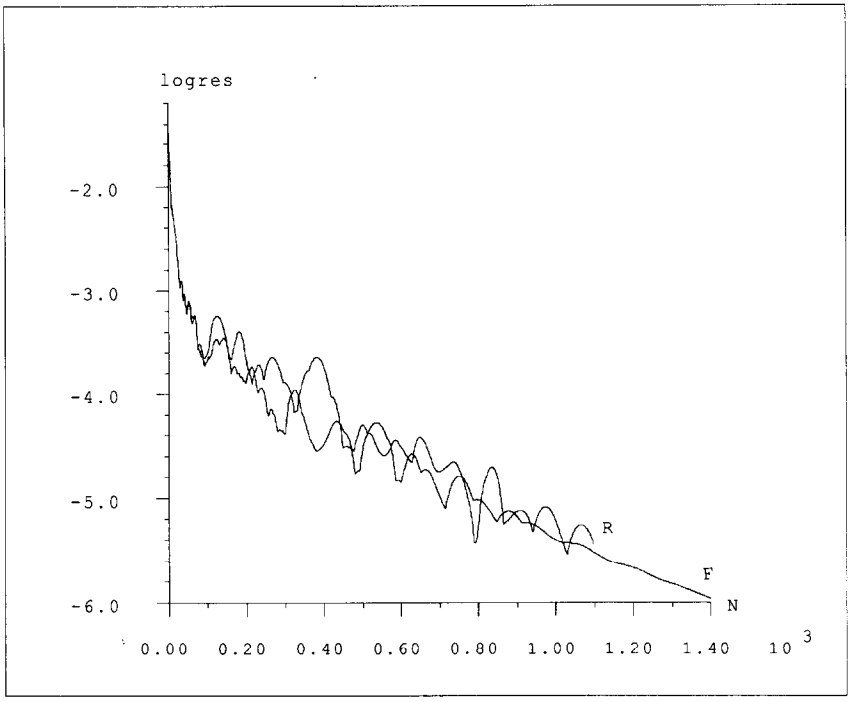

FIG. 5. Convergence history for the R-conditions with $r = 2.3$ and the F-conditions with $r = 13$.

another numerical method for the computations in the interior. No effort has been made to find a method which suits the boundary procedure well. The equations have just been solved with an available program.

We have just considered one test problem here. However, nothing is assumed about the configuration in the interior when the boundary conditions are constructed. The applicability for other configurations should thus mainly depend on the behavior of the solution outside the boundary. If, for example, the Mach number or angle of attack is changed, the size of the supersonic area should give a rough guideline to the choice of outer boundary.

5. CONCLUSIONS

Very accurate boundary conditions have been derived for the external problem in two space dimensions. The accuracy made it possible to reduce the radius of the computational region by a factor 5. By reducing the number of boundary condition points by a factor 4, the computational work at the boundary every time step could be kept low.

ACKNOWLEDGMENTS

I thank Professor Bertil Gustafsson for many valuable advise. The work has been supported financially by the Institute for Applied Mathematics, ITM, Stockholm, Sweden, and the Swedish Board for Technical Development.

REFERENCES

1. A. BAYLISS AND E. TURKEL, *J. Comput. Phys.* **48**, 182 (1982).
2. B. ENGQUIST AND A. MAJDA, *Math. Comput.* **31**, 629 (1977).
3. B. ENGQUIST AND A. MAJDA, *Commun. Pure Appl. Math.* **32**, 312 (1979).
4. L. FERM, *J. Comput. Phys.* **78**, 94 (1988).
5. L. FERM AND B. GUSTAFSSON, *Comput. Fluids* **10**, 261 (1982).
6. G. J. FIX AND S. P. MARIN, *J. Comput. Phys.* **28**, 253 (1978).
7. B. GUSTAFSSON, *SIAM J. Sci. Comput.* **9**, 812 (1988).
8. B. GUSTAFSSON AND H. O. KREISS, *J. Comput. Phys.* **30**, 333 (1979).
9. T. HAGSTROM AND H. B. KELLER, *SIAM J. Math. Anal.* **17**, 322 (1986).
10. A. RIZZI AND L. E. ERIKSSON, *J. Fluid. Mech.* **148**, 45 (1984).